Silicon (2022) 14:10807–10816
https://doi.org/10.1007/s12633-022-01782-9

ORIGINAL PAPER

Highly Stable APTES Incorporated CNTs Based Ternary Polymer Composites with Improved Dielectric and Thermal Properties

Tajamal Hussain[1] · Farrukh Bashir[1,2] · Adnan Mujahid[1] · Azeem Intisar[1] · Mirza Nadeem Ahmad[3] · Muhammad Aamir Raza[4] · Muhammad Imran Din[1] · Uzma Jabeen[2] · Ayesha Mushtaq[2] · Huma Tareen[2]

Received: 5 December 2021 / Accepted: 18 February 2022 / Published online: 19 March 2022

Abstract

High dielectric constant carbon nanotubes (CNTs) based polymer composites with enhanced thermal stability are promising materials for energy storage devices because of high breakdown voltage, ease in processing, enhanced flexibility and low cost. In the present work, 3-aminopropyltriethoxysilane (APTES) as additive was used along CNTs as filler and polymethylmethacrylate (PMMA) as matrix to enhance the dispersion of filler in matrix by increasing interfacial interaction between these two. These composites were synthesized by using solution casting method and monitored by FTIR spectroscopy whereas XRD and SEM analyses have been performed to explore the role of APTES in dispersion of CNTs. Significant improvement in the dielectric constant (Dielectric Constant: 40 at 1.6 wt% of CNTs) has been observed on adding small fraction of APTES-CNTs. An impressive increase in thermal stability of the composite was achieved because of APTES. It is noted that weight loss in APTES-CNTs/PMMA composite at 460 °C is less than that of CNTs/PMMA composite at 400 °C. Use of APTES-CNTs appears to be quite encouraging when the obtained values of dielectric constant and results of thermal stability of APTES-CNTs/PMMA are compared with those of pristine CNTs based PMMA (CNTs/PMMA) composites. Mechanism of APTES to control the agglomeration of CNTs in the composite is distinctive and effective in improving the features of composite.

Keywords Ternary polymer composites · High dielectric constant · Thermal stability · Energy storage

1 Introduction

Electroactive polymer composites with high dielectric constant value are considered as potential candidate for energy storage applications and actuators [1, 2]. Inorganic fillers based composites with high dielectric constant polymer matrix could be a suitable choice for this purpose [3, 4]. To obtain high net dielectric constant, large contents of such fillers are required which may increase the dielectric constant of polymer matrix but results in the loss of some important features of the polymer. More specifically, flexibility and ease in processing are compromised while fabricating the composites made up of inorganic based material as filler and high dielectric constant polymer matrix. On the other hand, composites fabricated from a high dielectric constant organic filler materials exhibit high net dielectric constant and also retained the flexibility of the matrix. Among different types of organic fillers, CNTs are recognized as excellent nanoscale filler with extra ordinary electrical and mechanical properties [5–7]. Different nanocomposites have been prepared by combining CNTs with different polymers like polystyrene (PS) or polyvinyl alcohol (PVA) [8, 9], but problem associated with the use of these CNTs, especially when used in large amount, is their agglomeration in polymer matrix which limits the features of electroactive polymer composites. Functionalization of CNTs is believed to be the best approach in order to reduce its agglomeration for example, surface modification, in-situ polymerization, chemical bonding [10, 11] etc. Modified CNTs are proved to be helpful in enhancing the electrical,

✉ Ayesha Mushtaq
ayeshamushtaq2000@yahoo.com

[1] School of Chemistry, University of the Punjab, Lahore 54590, Pakistan

[2] Department of Chemistry, Sardar Bahadur Khan Women's University Quetta, Quetta 87300, Pakistan

[3] Institute of Chemistry, Government College University, Faisalabad 38030, Pakistan

[4] Pakistan Council of Scientific and Industrial Research Laboratories Complex, Quetta 87300, Pakistan

thermal or mechanical properties of different polymers [12, 13]. CNTs modified by using organic polymer like polyaniline (PANI) and dodecyl benzene sulphonic acid (DBSA) are suggested to be helpful in enhancing the properties of polymethylmethacrylate (PMMA) by increasing the dispersion of CNTs in the matrix [14]. PMMA is a thermoplastic and shatter resistant polymer. Its excellent mechanical and optical properties make it useful in making its transparent thin films which can be used in number of applications in electronics. A lot of research has been done on the PMMA based composites by dispersing different fillers. However, much more work is required in order to explore its optical and dielectric properties.

In present work, (3-aminopropyl) triethoxysilane (APTES), coupling agent, was used along the CNTs for synthesis of PMMA composites (APTES-CNTs/PMMA). It is reported that after electrostatic adsorbing at the surface of the substrate, APTES undergoes self polymerization [15–17]. Researchers worked on PMMA and APTES combination for some different scientific aspects like in medical or for plastic binding [18, 19]. However, modification of CNTs by APTES for the enhancement of electrical and thermal properties of PMMA has not been studied yet. Here, it is expected that APTES would play its role in controlling the agglomeration of CNTs by developing the spread network in the matrix after adsorbing at the surface of CNTs and help in increasing the dielectric properties of the composites as reported [20]. Mechanism of controlling the agglomeration of CNTs by APTES is unique and effective one. Synthesis process of APTES-CNTs/PMMA was examined by FTIR spectrophotometer. To explore the role of APTES, scanning electron microscopy (SEM) and X-ray diffraction technique were employed. Values of the dielectric constant were measured as function of frequency and contents of CNTs with the help of LCR meter. Thermal stability of the composites was investigated by thermo gravimetric analysis (TGA). For better understanding of the role of APTES in APTES-CNTs/PMMA composites, their results were compared with those of pristine CNTs based PMMA composites (CNTs/PMMA).

2 Materials and Methods

PMMA (Molecular weight ~ 350,000), CNTs, 95% with O.D x L 6-9 nm × 5 μm and APTES (≥98%) were purchased from Sigma Aldrich while chloroform was obtained from Merck. All the chemicals were used as obtained without pretreatment.

2.1 Synthesis of CNTs/PMMA Composites

CNTs/PMMA composites with varied contents of CNTs were prepared by solution mixing method. For suspension of CNTs, calculated amount of CNTs was taken in 15 mL of chloroform and kept on stirring for one hour followed by ultra-sonication of 20 min. Separately prepared solution of calculated amount of PMMA in chloroform was added slowly in the homogeneous suspension of CNTs along vigorous stirring. Resultant blend was ultra-sonicated for 30 min. This blend was casted on petri dish and left at room temperature for evaporation of solvent to have thin film of CNTs/PMMA composites [21].

2.2 Formation of APTES-CNTs as Filler

CNTs were functionalized before treatment with APTES as reported in reference [22]. To prepare APTES-CNTs, a reported method [23] with some modification was used. Dispersion of equal weight of CNTs was mixed with 10% solution of APTES and resultant mixture was kept on stirring for 1 h followed by ultra-sonication of 1 h. APTES-CNTs were recovered and washed by distilled water and ethanol with the help of centrifugation.

2.3 Synthesis of APTES-CNTs/PMMA Composites

Above prepared filler, APTES-CNTs, was used in different amounts for the synthesis of APTES-CNTs/PMMA composites. For the preparation of 0.2 wt%, a weighed amount of APTES-CNTs was dispersed in 15 mL of chloroform at constant stirring of 1 h followed by ultrasonication for 20 min. This suspension was then added to a solution of PMMA dissolved in chloroform and kept for ultra-sonication for further 25 min. To get prepared composite in the form of thin film, this suspended solution was casted on petri dish and left overnight for the evaporation of solvent at room temperature. Same steps were followed for the preparation of other series of APTES-CNTs/PMMA composites by using prepared APTES-CNTs. Figure 1 shows the schematic steps followed during experiment. Detail of composition of the prepared composites is given in Table 1.

2.4 Instrumentations and Sample Preparations

FTIR spectra, of thin films of pure PMMA and its composites were recorded using FTIR spectrometer (CARY-630) of Agilent. For dielectric constant measurements, LCR meter (E4980AL) with frequency up to 1 MHz of Keysight Technologies was used. For analysis by FTIR spectrometer and LCR meter, squared shaped (sized: 1 in.) films of the composites and pure PMMA were directly used. For morphological study, Scanning Electron Microscope (S3700N) of Hitachi was used with a maximum acceleration voltage of 30 KV and magnification power ranges from 5× to 300Kx. Thermal stability was studied by using thermo gravimetric analyzer (TGA-50) of Shimadzu from room temperature to

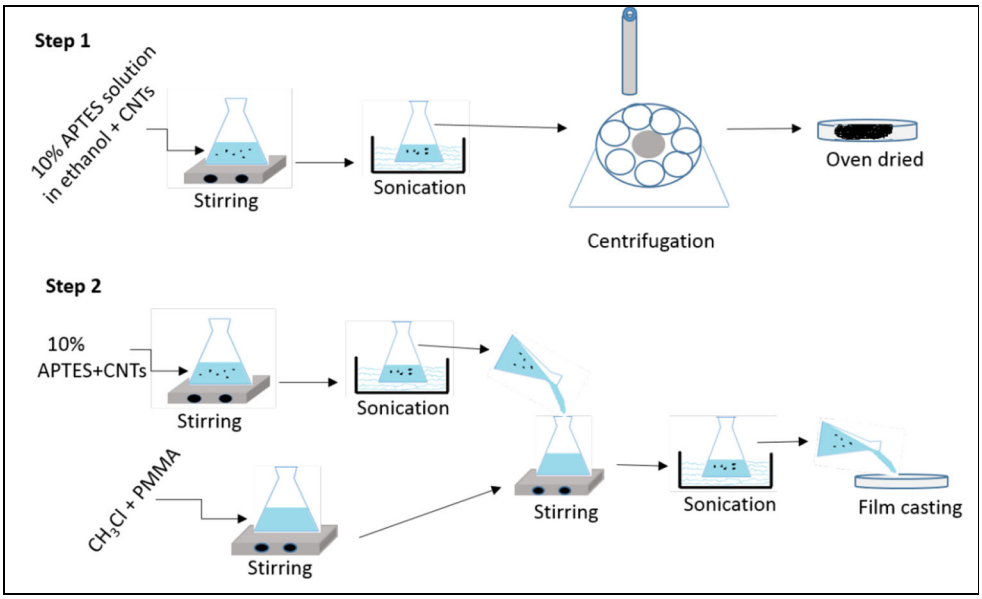

Fig. 1 Schematic steps followed during experimental analysis

600 °C under nitrogen atmosphere at heating rate of 20 °C min^{-1}.

3 Result and Discussion

3.1 Spectroscopic Characterization

Here, FTIR spectroscopy was performed to characterize the synthesized composites and APTES-CNTs. FTIR spectra of the thin films of pure PMMA, pure CNTs, APTES-CNTs, CNTs/PMMA and APTES-CNTs/PMMA composites at highest wt% of CNTs are given in Fig. 2. Usually, pure CNTs show no peak in IR spectrum as CNTs have no IR active species, however, the band appeared between 2000 and 2200 cm^{-1} represents the indirect CO_2 compensation from the atmosphere [24]. In the spectrum of APTES-CNTs, peaks appeared at 3355 cm^{-1} and 1621 cm^{-1} represent the stretching and deformation modes of $–NH_2$ [19, 25, 26], which do confirm the modification of APTES by CNTs. Spectrum of pure PMMA shows peaks around 1080 to 1199 cm^{-1} for bending vibration of C-O-C, peak at 1242 cm^{-1} for stretching vibration of C-O, low intensity peak at 1640 cm^{-1} corresponds –OH group bending vibration and peak at 1725 cm^{-1} belongs to stretching vibrations of C=O group [14, 27, 28]. In the spectrum of CNTs/PMMA no sharp change in the PMMA peaks are observed however, in case of APTES-CNTs/PMMA spectrum, an increase in the intensity of absorption band at 1640 cm^{-1} is observed which corresponds to the bending vibrations of $–NH_2$ group of APTES whereas, presence of additional low intensity peak at 3800 cm^{-1} belongs to the stretching vibrations, of $–NH_2$ group of APTES. Somehow, same results are reported in literature where PMMA surface was modified directly by APTES solution either to improve the adhesion between PMMA and skin tissue or bonding between polymers [18, 19]. Presence of peaks belonging to $–NH_2$ group of APTES indicates the incorporation of APTES-CNTs in PMMA, successful synthesis of APTES-CNTs/PMMA and peak pattern present in FTIR spectrum of PMMA is regenerated in the spectra of

Table 1 Wt% composition of CNTs, APTES and PMMA in CNTs/PMMA and APTES-CNTs/PMMA composites

S. No.	APTES-CNTs/PMMA			CNTs/PMMA	
	Wt.% of CNTs	Wt.% of APTES-CNTs	Wt.% of PMMA	Wt.% of CNTs	Wt.% of PMMA
1	0	0	100	0	100
2	0.4	0.8	99.6	0.05	99.95
3	0.6	1.2	98.8	0.1	99.9
4	0.8	1.6	98.4	0.5	99.5
5	1.4	2.8	97.2	0.63	99.37
6	1.6	3.2	96.8	1	99
7	2	4	96	1.47	98.53
8	2.5	5	95	2.31	97.69

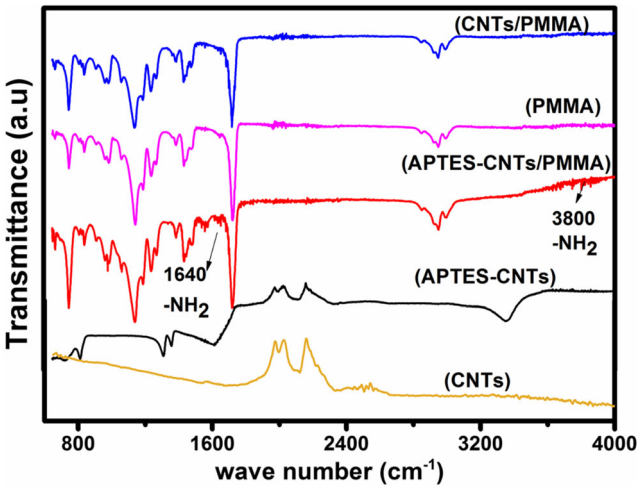

Fig. 2 FTIR spectra of pure PMMA, pure CNTs, APTES-CNTs, CNTs/PMMA and APTES-CNTs/PMMA composites at 2 wt% of CNTs

CNTs/PMMA and APTES-CNTs/PMMA composites which indicates that chemical structure of the PMMA is remained intact after the composite formation [29].

3.2 Structural and Morphological Studies

X-ray diffractogram of CNTs, APTES-CNTs, PMMA, CNTs/PMMA and APTES-CNTs/PMMA are shown in Fig. 3. Main humps of PMMA are present in all the three types of diffractograms. XRD of CNTs shows single peak at 25.6 ° as reported in literature [30–32] which is regenerated in CNTs/PMMA composite as well. Moreover, in case of APTES-CNTs/PMMA, two noticeable changes occur; slight change in shape of humps and disappearance of peak that belongs to CNTs. Latter is due to better dispersion of CNTs and former is probably because of coupling of APTES with PMMA. This supports our stance for use of APTES to

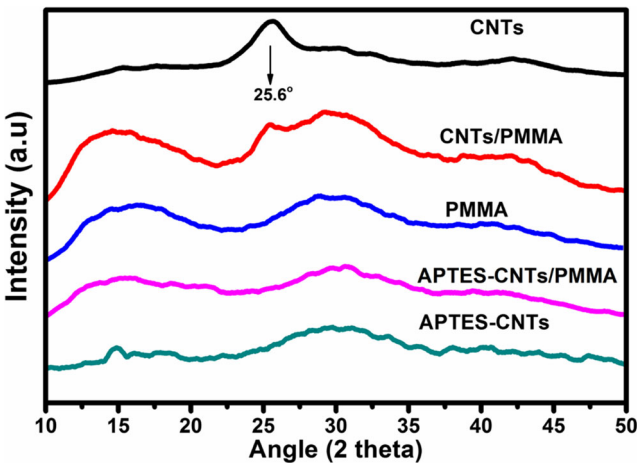

Fig. 3 X-ray diffractogram patterns of CNTs, PMMA, APTES-CNTs, CNTs/PMMA composite with 2.3 wt% of CNTs and APTES-CNTs/PMMA composite with 2.5 wt% of CNTs

enhance dispersion of CNTs by establishing spread network in PMMA.

Figure 4 shows the SEM images with surface profile and topography of the APTES-CNTs/PMMA and CNTs/PMMA composites. The morphology of composite surfaces demonstrates the effect of the presence or absence of APTES on the dispersion of CNTs in the PMMA matrix. In the absence of APTES, CNTs are dispersed in the form of stacks of random sizes with uneven distribution, as shown in Fig. 4c, d. On the other hand, APTES presence results in the homogeneous distribution of the CNTs in the whole structure of PMMA and thus, forms a uniformly patterned surface, as shown in Fig. 4a, b.

The topographic analyses of the respective micrographs exhibits critical differences in the surface properties of APTES-CNTs/PMMA and CNTs/PMMA composites, which are summarized in Table 2. The average and root-mean-square (RMS) roughness of APTES-CNTs/PMMA and CNTs/PMMA composites are comparable, but the standard deviation values are quite different which is emphasizing the morphological differences. The uniformity of surface features in APTES-CNTs/PMMA composite is demonstrated by the very low standard deviation, while CNTs/PMMA composite surface shows inhomogeneity with high standard deviation and inconsistent distribution of peaks and valleys.

3.3 Dielectric Properties

Dielectric constant calculated using Eq. 1 [33] as function of wt% of CNTs for both types of composites are presented in Fig. 7.

$$\varepsilon_r = \frac{t_m\, c}{\pi\left(\frac{d}{2}\right)^2 \varepsilon_\circ} \tag{1}$$

Where C is capacitance of dielectric material, d is diameter of the electrodes (0.001 m), t_m is thickness of the sample (0.0001 m) and ε_o is free space permittivity (8.854×10^{-12} F/m). Dielectric constant of the PMMA is found to be significantly improved on addition of small amount of CNTs for both types of composites. Maximum values of dielectric constant as high as 40 and 25 are observed for APTES-CNTs/PMMA and CNTs/PMMA composites respectively, with just 1.6 wt% of CNTs. Interface of CNTs and PMMA results in the development of nano capacitors which becomes the reason for the accumulation of electrical charges [34]. Higher are the contents of scattered CNTs, higher will be interfacial surface. Thus, higher accumulated charges result in an enhanced value of dielectric constant.. Recently, Adaptive Neuro Fuzzy Inference System (ANFIS) was used for the functionalization of CNTs in order to obtain the high dielectric constant value of PMMA composites. However, the maximum value obtained by using this approach was only 12 [35]. But here, significantly improved value of dielectric constant for APTES-CNTs/PMMA as compared to

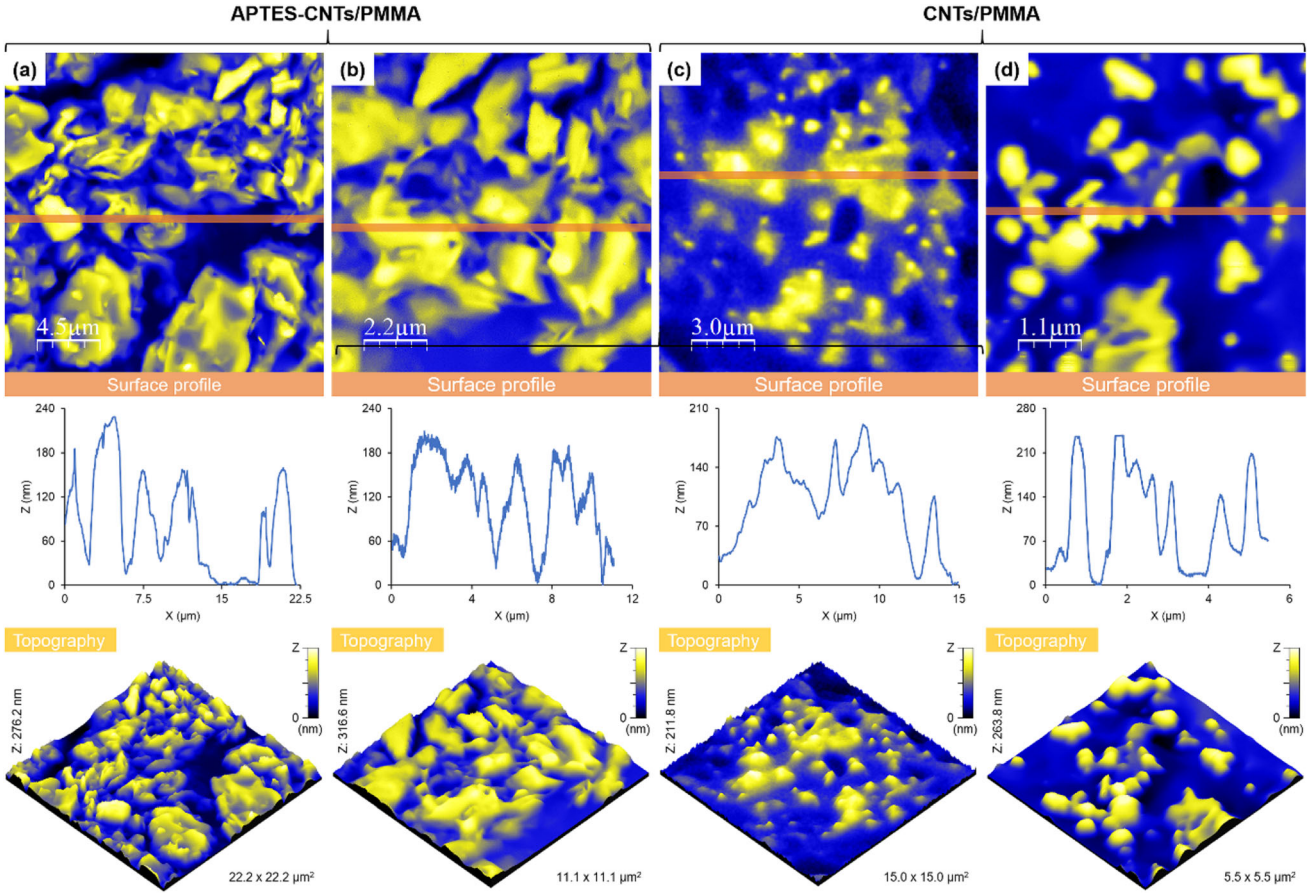

Fig. 4 SEM images, surface profile of the selected area (highlighted in grey), and 3d-micrographs of **a**-**b** APTES-CNTs/PMMA, and **c**-**d** CNTs/PMMA composites at highest wt% of CNTs

that of CNTs/PMMA and other PMMA based composites reported in literature is obtained due to enhanced dispersion of CNTs in PMMA because of APTES. Thus, networking by APTES keeps the CNTs apart and results in high population of charge accumulated in the APTES-CNTs/PMMA composite.

Dielectric constant as function of frequency for APTES-CNTs/PMMA composites with different wt% of CNTs is displayed in Fig. 5b and response of dielectric constant to frequency is observed to be quite interesting. Dependence of dielectric constant on frequency for composites with 1.6 wt% of CNTs is strongest one. Refer to Fig. 5a, value of dielectric constant observed is maximum for APTES-CNTs/PMMA composite with 1.6 wt% of CNTs. According to percolation theory, it can be assumed that percolation network would be formed for composites with higher contents of CNTs and thus results drop in of value of dielectric constant. Strong frequency dependence of dielectric constant for composite with 1.6 wt% of CNTs suggests the presence of maximum charge polarization as a result of accumulation of charges at the interface of CNTs and PMMA at this point [36–39]. This kind of materials is considered as the best choice for actuators [40]. Here, APTES helped in having large value of dielectric constant before establishing the conductive network and significant frequency dependent dielectric constant.

Table 2 The surface properties of APTES-CNTs/PMMA and CNTs/PMMA composites

Surface properties	APTEs-CNTs/PMMA		CNTs/PMMA	
	Average value	Standard deviation	Average value	Standard deviation
RMS roughness (nm)	58.33	3.57	58.87	18.71
Average roughness (nm)	49.57	3.37	47.93	15.03
Average height (nm)	137.0	21.4	105.2	34.8
Maximum height (nm)	284.6	28.8	265.9	55.1

Table note. The surface properties are determined from the topographic analysis of at least three SEM micrographs of composite surfaces with different magnifications

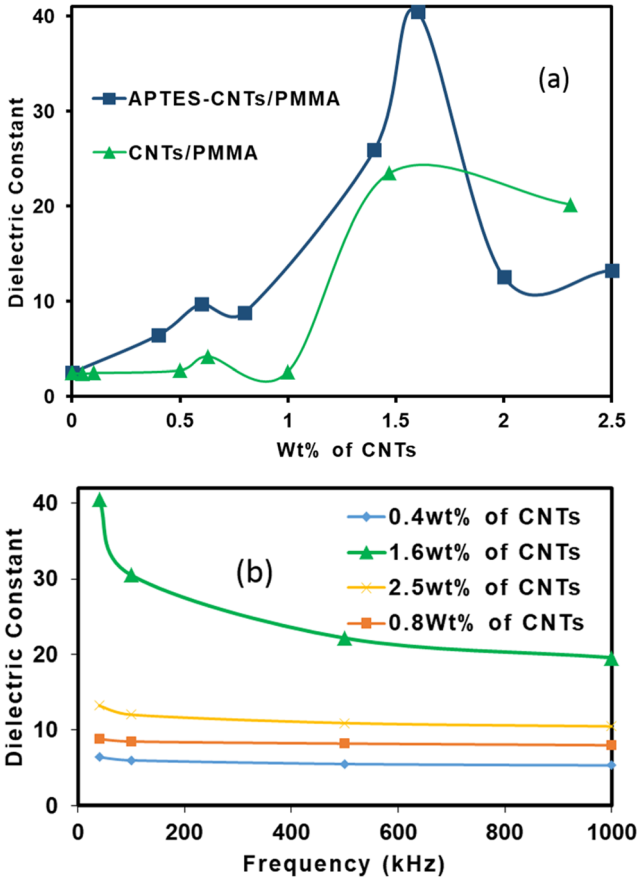

Fig. 5 **a** Trend of dependence of dielectric constant on contents of CNTs for APTES-CNTs/PMMA and CNTs/PMMA composites. **b** Frequency dependence of dielectric constant for APTES-CNTs/PMMA composites with different contents of CNTs

3.4 Electrical Percolation and Conductivity

Study of electrical percolation phenomena is considered as vital factor in establishing electrical character of polymer composites used in electronics. Electrical percolation phenomena can be well explained by simple power law given in Eq. 2 [41]

$$\sigma \ \alpha \ (f-f_c)^t \quad for \quad f \geq f_c \tag{2}$$

Where σ ιs conductivity, f is the filler content, f_c *is* critical amount of filler at percolation threshold and t is the exponent constant. A linear log-log plot of (f-fc) against σ is used to determine the values of "f_c" and "t". Insets of Fig. 6a, b represent these linear plots for CNTs/PMMA and APTES-CNTs/PMMA composites, respectively. Calculated values of f_c and t are 0.05 wt.% and 1.2, respectively, for APTES-CNTs/PMMA composites and 0.5 wt.% and 2, respectively, for CNTs/PMMA composites. Universal value of "t" with three dimensional system reported in the literature [42] is well matched with present work. Values of percolation threshold reported in literature for CNTs based PMMA composite are given in Table 3. Here, low value of percolation threshold was obtained in case of APTES-CNTs/PMMA than CNTs/PMMA and similar reported composites. It is reported elsewhere that APTES functionalized at the surface of polymer immobilized the biomolecule dispersed at the polymeric surface [25]. Likewise, it is supposed that APTES reduces the mobilization of the CNTs which restrict the re-agglomeration of CNTs. Therefore, better dispersion of CNTs becomes the reason of low value of percolation threshold. SEM images given in Fig. 4 also support the claim of more uniform and homogeneous dispersion of CNTs in APTES-CNTs/PMMA than in CNTs/PMMA composites.

Figure 6a, b show the electrical conductivities of CNTs/PMMA and APTES-CNTs/PMMA composites as function of CNTs at 1000 KHz. It is observed that addition of small amount of CNTs in PMMA increases the conductivity of the composites significantly. Seven to eight orders of magnitude increase in conductivity is observed on addition of 0.8 wt% and 1 wt% of CNTs with and without APTES, respectively. Similarly, maximum value of conductivity was found in the order of 10^{-1} S/cm for both types of composites with contents of CNTs range from 1.8–2 wt% with APTES and 2–2.2 wt% without APTES. Data of maximum conductivity along with contents of CNTs at which this value was obtained from literature for CNTs based PMMA composites is given in Table 3. It can be noticed that there are only two cases where values of maximum conductivity recorded are greater

Table 3 Data of electrical properties and method of preparation of CNTs based PMMA composites

Sr. No.	σ_{max} (S/cm)	f_c	*ε	State of the CNTs	Method of preparation	Ref
1	1.37 (10 vol%)	0.5 wt%	–	Pristine CNTs	Solution mixing method	[43]
2	10^{-2} (3 wt%)	0.07 wt%	–	PEO modified CNTs	Two step solution mixing method	[44]
3	10^{-6} (1 wt%)	1.52 wt%		Very high aspect ratio CNTs	Melt mixing method	[45]
4	10 (40 wt%)	0.3%	–	CNTs with Fe as catalyst	Solution mixing method	[46]
5	≈10^{-3} (5 wt%)	0.5 wt%	–	Modified CNTs with acyl group	Solution mixing method	[47]
6	10^{-1} (1.5 wt%)	0.1 wt%	10 (2 wt%)	PS adsorbed CNTs	Solution mixing method	[48]
7	5 X10^{-4} (10 wt%)	8.5 wt%	12 (10 wt%)	Pristine CNTs	Melt mixing method	[49]

*ε = dielectric constant

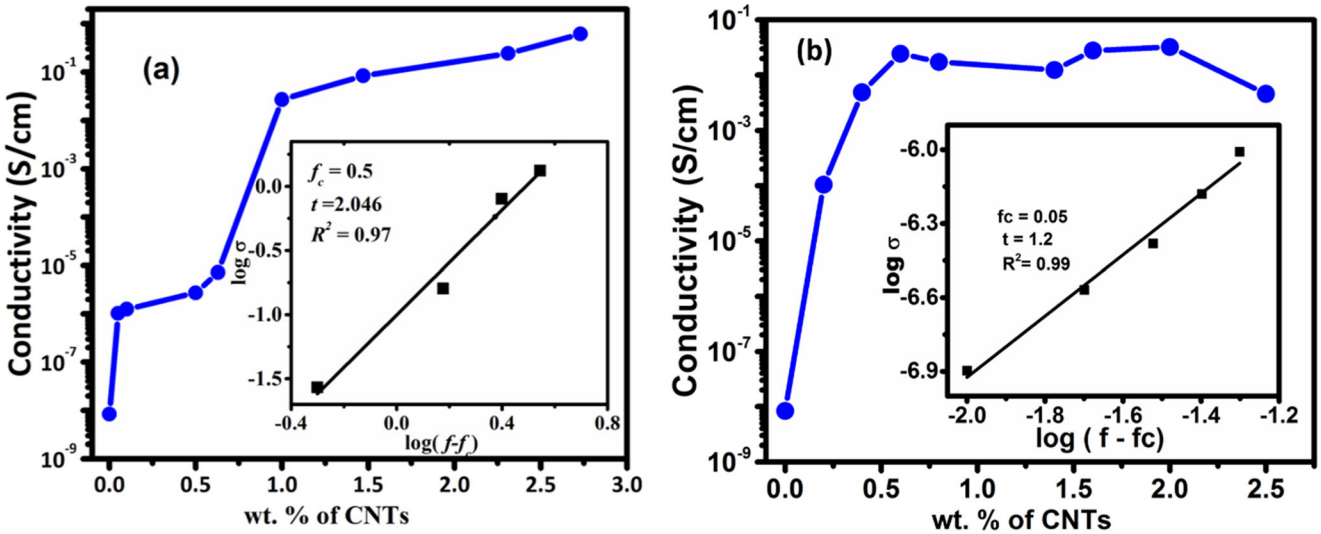

Fig. 6 Electrical conductivity of **a** CNTs/PMMA, and **b** APTES-CNTs/PMMA composites

than value observed in present work. At one place [43], pristine CNTs were used which resulted high value of maximum conductivity but at significantly large filler contents. In second case, Fe adsorbed at the surface of CNTs were used as filler and thus, Fe, additionally, contributed towards observed conductivity value [50]. But, as already discussed, use of inorganic fillers results in suppression of other important features of polymer. A low value of percolation threshold and achievement of maximum conductivity at relatively low wt% of CNTs for APTES-CNTs/PMMA is become possible because of the enhanced dispersion of CNTs due to spread network of APTES which not only helps in developing indirect interaction between CNTs and PMMA but also set CNTs apart from each other by reducing the chances of their interaction. Thus, because of the dual role of APTES, significantly enhanced value of dielectric constant, conductivity and improved percolation threshold are obtained.

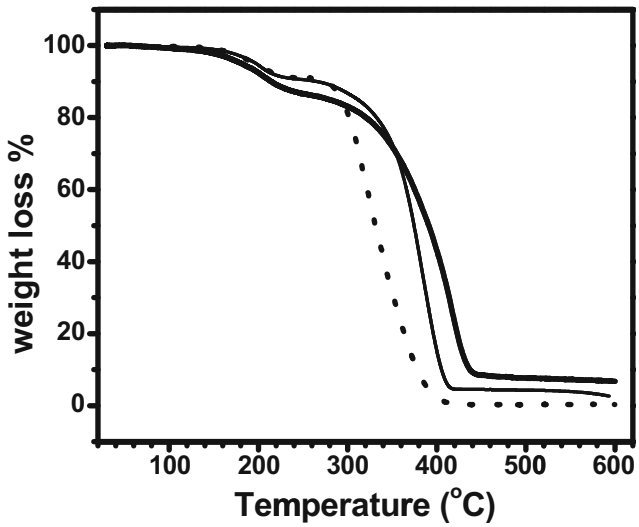

Fig. 7 Plot of thermal degradation of PMMA (dotted line), CNTs/PMMA (thin line) and APTES-CNTs/PMMA (thick line) composites at highest wt% of CNTs

3.5 Thermal Stability

Thermal stability of the prepared composites and PMMA was investigated by thermal gravimetric analyzer and results of thermal degradation are given in Fig. 7. Almost 3% of CNTs/PMMA and 7% of APTES-CNTs/PMMA composites were left at 600 °C but PMMA was decomposed completely at 400 °C. Amount of APTES-CNTs/PMMA composites left at 460 °C was greater than that of CNTs/PMMA composites at 400 °C. Comparison of the thermal stability of APTES-CNTs/PMMA composites with that of CNTs/PMMA composites and similar systems found in literature encourages the use of APTES [51].

Decomposition start, mid and end temperatures along with char yield, are shown in Table 4. In order to show the increase in thermal stability of APTES-CNTs/PMMA composite, heat resistance index (T_{HRI}) was calculated for both types of composites by using the following equation [52] and are given in Table 4.

$$T_{HRI} = 0.49 \times [T_5 + 0.6 \times (T_{30} - T_5)] \quad (3)$$

Here T_5 and T_{30} represent temperature values at which 5% and 30% of weight losses were occurred, respectively. Increasing order of T_{HRI} from PMMA to CNTs/PMMA and followed by APTES-CNTs/PMMA is shown in Table 4. As reported in literature an increase in T_{HRI} increases the thermal stability [53, 54], therefore, thermal stability of APTES-CNTs/PMMA composite is found to be more as compared to CNTs/PMMA and PMMA. Galip and his co-workers synthesized microcapsules of PMMA filled with CNTs and

Table 4 Decomposition temperature at different stages with char yield % and heat resistance index of PMMA and composites of CNTs/PMMA and APTES-CNTs/PMMA

Sample	Decomposition			Char yield (%) at 593 °C	T_5 (°C)	T_{30} (°C)	T_{HRI} (°C)
	Start (°C)	Mid (°C)	End (°C)				
PMMA	29.87	330.4	600	0.34	389.15	351.46	179.6
CNTs/PMMA	36.85	376.23	593	2.67	415	388.7	195.6
APTES-CNTs/PMMA	39.6	384	600	6.7	>600	413.94	>239.3

epoxy resin and maximum T_{HRI} calculated for their mixture was 151.46 °C [52] which is significantly low as compared to the present work. Moreover, in Fig. 7 it is clearly observed that APTES-CNTs/PMMA remained stable even at instrumental maximum temperature i.e., 600 °C with 6.7% residue. Therefore, the calculated T_{HRI} value is also expected to be greater than 239.3 °C which is significantly higher than both PMMA and CNTs/PMMA. This higher value of T_{HRI} reflects that APTES not only reduced the agglomeration of CNTs by adsorbing at its surface but also helped in increasing the resistant ability of PMMA against the flow of heat.

4 Conclusion

Successful syntheses of APTES-CNTs/PMMA and CNTs/PMMA composites have been reported and monitored by FTIR spectroscopy. As confirmed by XRD study and SEM analysis, APTES helped in having composites with uniform dispersion of CNTs. Significant improvement in dielectric properties particularly maximum value (40) of dielectric constant has been achieved for organic filler based PMMA composites. Conductivity value obtained for both APTES-CNTs/PMMA and CNT/PMMA composites was around 10^{-1} S/cm. Results of thermal stability like other characterization techniques are in the favour of use of APTES along CNTs for synthesis of composites.

Acknowledgements Tajamal Hussain acknowledges University of Punjab, Lahore, for financial support to carry out this research work through research project (PU Research Grant 2017-18).

Authors' Contributions All authors contributed to the study conception and design. Farrukh Bashir designed and performed all the experiments in University of Punjab, Lahore. All the facilities and guidance for SEM, BET, FTIR analysis were provided by Tajamal Hussain in University of Punjab, Lahore. The research was supervised and the original idea was conceived by Tajamal Hussain and Adnan Mujahid. Azeem Intisar, Mirza Nadeem Ahmad, Muhammad Aamir Raza and Muhammad Imran Din processed the experimental data, performed the analysis and finalized the manuscript with support from all other authors. All the authors read and approved the final manuscript agreed to the sequence of authorship and for publication of this research in Silicon Journal.

Data Availability Not applicable.

Declaration

Competing Interests The authors declare that they have no known competing financial interests or personal relationships that could have appeared to influence the work reported in this paper.

Ethics Approval We confirm that all authors consent to ethical standards.

Informed Consent Not applicable.

Consent to Participate Not applicable.

Competing Interests Authors declare there have no conflicts of interest.

References

1. Tang L, He M, Na X, Guan X, Zhang R, Zhang J, Junwei G (2019) Functionalized glass fibers cloth/spherical BN fillers/epoxy laminated composites with excellent thermal conductivities and electrical insulation properties. Compos Commun 16:5–10. https://doi.org/10.1016/j.coco.2019.08.007
2. Zhang R-H, Shi X-T, Lin T, Zheng L, Zhang J-L, Guo Y-Q, Jun-Wei G (2020) Thermally conductive and insulating epoxy composites by synchronously incorporating Si-sol functionalized glass fibers and boron nitride fillers. Chin J Polym Sci 38(7):730–739
3. Ameen Khan M, Madhu GM, Sailaja RRN (2021) Polymethyl methacrylate reinforced with nickel coated multi-walled carbon nanotubes: flame, electrical and mechanical properties. Polym Compos 42(1):498–511
4. Zhang QM, Li H, Poh M, Feng X, Cheng Z-Y, Xu H, Cheng H (2002) An all-organic composite actuator material with a high dielectric constant. Nature 419(6904):284–287
5. Habisreutinger SN, Leijtens T, Eperon GE, Stranks SD, Nicholas RJ, Snaith HJ (2014) Carbon nanotube/polymer composites as a highly stable hole collection layer in perovskite solar cells. Nano Lett 14(10):5561–5568
6. Martin DC, Abidian MR (2015) Conducting polymer nanotube actuators for precisely controlled release of medicine and bioactive molecules. Google Patents
7. Zeng Z, Jin H, Zhang L, Zhang H, Chen Z, Gao F, Zhang Z (2015) Low-voltage and high-performance electrothermal actuator based on multi-walled carbon nanotube/polymer composites. Carbon 84:327–334
8. Al-Saleh MH (2019) Synergistic effect of CNT/CB hybrid mixture on the electrical properties of conductive composites. Mater Res Express 6(6):065011

9. Yeung, Raymond, Xiaobo Zhu, Terence Gee, Ben Gheen, David Jassby, and Victor GJ Rodgers. 2020. "Single and binary protein electroultrafiltration using poly (vinyl-alcohol)-carbon nanotube (PVA-CNT) composite membranes." PLoS One 15 (4):e0228973
10. Liu H, Tang Y, Jin Z, Song S, Zhang P, Zhao S, Guan S, Guan W (2020) Surface functionalization of carbon nanotubes by biological adhesive polymers carbopol for developing high-permittivity polymer composites. J Vinyl Addit Technol 26(2):165–172
11. Naqvi STR, Rasheed T, Hussain D, ul Haq MN, Majeed S, Shafi S, Ahmed N, Nawaz R (2020) Modification strategies for improving the solubility/dispersion of carbon nanotubes. J Mol Liq 297: 111919. https://doi.org/10.1016/j.molliq.2019.111919
12. Huang Y, Ellingford C, Bowen C, McNally T, Wu D, Wan C (2020) Tailoring the electrical and thermal conductivity of multicomponent and multi-phase polymer composites. Int Mater Rev 65(3):129–163
13. Yang Y, Li L-y, Yin B, Yang M-b (2020) An effective strategy to achieve ultralow electrical percolation threshold with CNTs anchoring at the Interface of PVDF/PS bi-continuous structures to form an interfacial conductive layer. Macromol Mater Eng 305(4):1900835
14. Bashir F, Hussain T, Mujahid A, Shehzad K, Raza MA, Zahid M, Athar MM (2017) Tailoring electrical and thermal properties of polymethyl methacrylate-carbon nanotubes composites through polyaniline and dodecyl benzene sulphonic acid impregnation. Polym Compos 39(S2):E1052–E1059
15. Acres RG, Ellis AV, Alvino J, Lenahan CE, Khodakov DA, Metha GF, Andersson GG (2012) Molecular structure of 3-aminopropyltriethoxysilane layers formed on silanol-terminated silicon surfaces. J Phys Chem C 116(10):6289–6297
16. Meroni D, Presti LL, Di Liberto G, Ceotto M, Acres RG, Prince KC, Bellani R, Soliveri G, Ardizzone S (2017) A close look at the structure of the TiO2-APTES Interface in hybrid nanomaterials and its degradation pathway: an experimental and theoretical study. J Phys Chem C 121(1):430–440. https://doi.org/10.1021/acs.jpcc.6b10720
17. Vandenberg ET, Bertilsson L, Liedberg B, Uvdal K, Erlandsson R, Elwing H, Lundström I (1991) Structure of 3-aminopropyl triethoxy silane on silicon oxide. J Colloid Interface Sci 147(1): 103–118
18. Riau AK, Mondal D, Yam GHF, Setiawan M, Liedberg B, Venkatraman SS, Mehta JS (2015) Surface modification of PMMA to improve adhesion to corneal substitutes in a synthetic core–skirt keratoprosthesis. ACS Appl Mater Interfaces 7(39): 21690–21702
19. Vlachopoulou ME, Tserepi A, Pavli P, Argitis P, Sanopoulou M, Misiakos K (2008) A low temperature surface modification assisted method for bonding plastic substrates. J Micromech Microeng 19(1):015007
20. Zhang X, Zheng J, Xu L, Yin M, Zhang G, Zhao W, Zhang Z, Shen C, Meng Q (2021) Novel thin film nanocomposite forward osmosis membranes prepared by organic phase controlled interfacial polymerization with functional multi-walled carbon nanotubes. Membranes 11(7):476
21. Tomar AK, Mahendia S, Kumar S (2011) Structural characterization of PMMA blended with chemically synthesized PAni. Adv Appl Sci Res 2(3):327–333
22. Lin Y, Rao AM, Sadanadan B, Kenik EA, Sun Y-P (2002) Functionalizing multiple-walled carbon nanotubes with aminopolymers. J Phys Chem B 106(6):1294–1298
23. Yu L, Li CM, Zhou Q, Gan Y, Bao QL (2007) Functionalized multi-walled carbon nanotubes as affinity ligands. Nanotechnology 18(11):115614
24. Lavagna L, Massella D, Pavese M (2017) Preparation of hierarchical material by chemical grafting of carbon nanotubes onto carbon fibers. Diam Relat Mater 80:118–124
25. Hsiao VKS, Waldeisen JR, Zheng Y, Lloyd PF, Bunning TJ, Huang TJ (2007) Aminopropyltriethoxysilane (APTES)-functionalized nanoporous polymeric gratings: fabrication and application in biosensing. J Mater Chem 17(46):4896–4901
26. Majoul N, Aouida S, Bessaïs B (2015) Progress of porous silicon APTES-functionalization by FTIR investigations. Appl Surf Sci 331:388–391
27. Duan G, Zhang C, Li A, Yang X, Lu L, Wang X (2008) Preparation and characterization of mesoporous zirconia made by using a poly (methyl methacrylate) template. Nanoscale Res Lett 3(3):118–122. https://doi.org/10.1007/s11671-008-9123-7
28. Requena S, Lacoul S, Strzhemechny YM (2014) Luminescent properties of surface functionalized BaTiO3 embedded in poly (methyl methacrylate). Materials 7(1):471–483
29. Gayen AL, Paul BK, Roy D, Kar S, Bandyopadhyay P, Basu R, Das S, Bhar DS, Manchanda RK, Khurana AK (2017) Enhanced dielectric properties and conductivity of triturated copper and cobalt nanoparticles-doped PVDF-HFP film and their possible use in electronic industry. Mater Res Innov 21(3):166–171
30. Al-Kahtani AA, Almuqati T, Alhokbany N, Ahamad T, Naushad M, Alshehri SM (2018) A clean approach for the reduction of hazardous 4-nitrophenol using gold nanoparticles decorated multiwalled carbon nanotubes. J Clean Prod 191:429–435. https://doi.org/10.1016/j.jclepro.2018.04.197
31. Badawi A, Al Hosiny N (2015) Dynamic mechanical analysis of single walled carbon nanotubes/polymethyl methacrylate nanocomposite films. Chin Phys B 24(10):105101
32. Ramoraswi N, Ndungu P (2015) Photo-catalytic properties of TiO2 supported on MWCNTs, SBA-15 and silica-coated MWCNTs nanocomposites. Nanoscale Res Lett 10:427. https://doi.org/10.1186/s11671-015-1137-3
33. Sannakki B (2013) Dielectric properties of PMMA and its composites with ZrO2. Phys Procedia 49:15–26
34. Babu K, Prasanna Kumar TS (2012) Optimum CNT concentration and bath temperature for maximum heat transfer rate during quenching in CNT nanofluids. J ASTM Int 9(5):1–12
35. Deep N, Mishra P, Das L (2020) Application of adaptive neuro-fuzzy inference system (ANFIS) for predicting dielectric characteristics of CNT/PMMA nanocomposites. Mater Today Proc 33: 5200–5205
36. Lim E, Manaka T, Tamura R, Iwamoto M (2006) Maxwell–Wagner model analysis for the capacitance–voltage characteristics of pentacene field effect transistor. Jpn J Appl Phys 45(4S):3712–3716
37. Macutkevic J, Kuzhir P, Paddubskaya A, Shuba M, Banys J, Maksimenko S, Kuznetsov VL, Mazov IN, Krasnikov DV (2013) Influence of carbon-nanotube diameters on composite dielectric properties. Phys Status Solidi A 210(11):2491–2498
38. Shehzad K, Dang Z-M, Ahmad MN, Sagar RUR, Butt S, Farooq MU, Wang T-B (2013) Effects of carbon nanotubes aspect ratio on the qualitative and quantitative aspects of frequency response of electrical conductivity and dielectric permittivity in the carbon nanotube/polymer composites. Carbon 54:105–112
39. Tamura R, Lim E, Manaka T, Iwamoto M (2006) Analysis of pentacene field effect transistor as a Maxwell-Wagner effect element. J Appl Phys 100(11):114515
40. Thomas P, Ravindran RSE, Varma KBR (2012) "Dielectric properties of Poly (methyl methacrylate)(PMMA)/CaCu 3 Ti 4 O 12 composites." 2012 IEEE 10th International Conference on the Properties and Applications of Dielectric Materials
41. Dang Z-M, Shehzad K, Zha J-W, Hussain T, Jun N, Bai J (2011a) On refining the relationship between aspect ratio and percolation threshold of practical carbon nanotubes/polymer nanocomposites. Jpn J Appl Phys 50(8R):080214
42. Dang Z-M, Shehzad K, Zha J-W, Mujahid A, Hussain T, Nie J, Shi C-Y (2011b) Complementary percolation characteristics of carbon

fillers based electrically percolative thermoplastic elastomer composites. Compos Sci Technol 72(1):28–35
43. Mathur RB, Shailaja P, Singh BP, Dhami TL (2008) Electrical and mechanical properties of multi-walled carbon nanotubes reinforced PMMA and PS composites. Polym Compos 29(7):717–727
44. Mir SM, Jafari SH, Khonakdar HA, Krause B, Pötschke P, Qazvini NT (2016) A promising approach to low electrical percolation threshold in PMMA nanocomposites by using MWCNT-PEO predispersions. Mater Des 111:253–262
45. McClory C, McNally T, Baxendale M, Pötschke P, Blau W, Ruether M (2010) Electrical and rheological percolation of PMMA/MWCNT nanocomposites as a function of CNT geometry and functionality. Eur Polym J 46(5):854–868
46. Kim HM, Kim K, Lee CY, Joo J, Cho SJ, Yoon HS, Pejaković DA, Yoo J-W, Epstein AJ (2004) Electrical conductivity and electromagnetic interference shielding of multiwalled carbon nanotube composites containing Fe catalyst. Appl Phys Lett 84(4):589–591
47. Huang Y-L, Yuen S-M, Ma C-CM, Chuang C-Y, Yu K-C, Teng C-C, Tien H-W, Chiu Y-C, Wu S-Y, Liao S-H (2009) Morphological, electrical, electromagnetic interference (EMI) shielding, and tribological properties of functionalized multi-walled carbon nanotube/poly methyl methacrylate (PMMA) composites. Compos Sci Technol 69(11–12):1991–1996
48. Hussain T, Malik T, Mujahid A, Mustafa G (2018) Polystyrene adsorbed multi-walled carbon nanotubes incorporated polymethylmethacrylate composites with modified percolation phenomena. MRS Adv 3(1–2):25–30
49. Khattari Z, Maghrabi M, McNally T, Jawad SA (2012) Impedance study of polymethyl methacrylate composites/multi-walled carbon nanotubes (PMMA/MWCNTs). Phys B Condens Matter 407(4): 759–764
50. Hussain T, Jabeen S, Shehzad K, Mujahid A, Ahmad MN, Farooqi ZH, Raza MH (2016) Polyaniline/silver decorated-MWCNT composites with enhanced electrical and thermal properties. Polym Compos 39(S3):E1346–E1353
51. Tigelaar DM, Meador MAB, Kinder JD, Bennett WR (2006) New APTES cross-linked polymers from poly (ethylene oxide) s and cyanuric chloride for lithium batteries. Macromolecules 39(1): 120–127
52. Icduygu, M Galip, Meltem Asilturk, M Akif Yalcinkaya, Youssef K Hamidi, and M Cengiz Altan. 2019. "Three-dimensional nanomorphology of carbon nanotube/epoxy filled poly (methyl methacrylate) microcapsules." Materials 12 (9):1387
53. Lin T, Zhang J, Junwei GU (2021) Random copolymer membrane coated PBO fibers with significantly improved interfacial adhesion for PBO fibers/cyanate ester composites. Chin J Aeronaut 34(2): 659–668
54. Zhao J, Zhang J, Wang L, Li J, Feng T, Fan J, Chen L, Junwei G (2020) Superior wave-absorbing performances of silicone rubber composites via introducing covalently bonded SnO2@ MWCNT absorbent with encapsulation structure. Compos Commun 22: 100486